

**The use of polymer blends to improve stability and performance of electrospun solid dispersions: the role of miscibility and phase separation**

Pratchaya Tipduangta<sup>1,3</sup>, Peter Belton<sup>2</sup>, William J. McAuley<sup>4</sup>

and Sheng Qi<sup>1\*</sup>

<sup>1</sup>School of Pharmacy, University of East Anglia, Norwich, Norfolk, UK, NR4 7TJ

<sup>2</sup>School of Chemistry, University of East Anglia, Norwich, Norfolk, UK, NR4 7TJ

<sup>3</sup>Department of Pharmaceutical Science, Faculty of Pharmacy, Chiang Mai University,  
Chiang Mai, Thailand 50200

<sup>4</sup>Centre for Research in Topical Drug Delivery and Toxicology, School of Life and  
Medical Sciences, University of Hertfordshire, College Lane, Hatfield, AL10 9AB,  
UK

Correspondence: Sheng Qi, [sheng.qi@uea.ac.uk](mailto:sheng.qi@uea.ac.uk)

Tel: +44 (0)1603592925; Fax: +44 (0)1603592003

## **Abstract**

Solid dispersion-based nanofiber formulations of poorly soluble drugs prepared by electrospinning (ES) with a water-soluble polymer, can offer significant improvements in drug dissolution for oral drug administration. However, when hygroscopic polymers, such as polyvinylpyrrolidone (PVP) are used, environmental moisture sorption can lead to poor physical stability on storage. This study investigated the use of polymer blends to modify PVP-based ES formulations of a model poorly soluble drug, fenofibrate (FF), to improve its physical stability without compromising dissolution enhancement. FF-PVP ES dispersions demonstrated clear dissolution enhancement, but poor storage stability against high humidity. Polymer blends of PVP with Eudragit E PO, Soluplus and hypromellose acetate succinate (HPMCAS), were selected because of the low intrinsic moisture sorption of these polymers. The drug-polymer and polymer-polymer miscibility study revealed that FF was more miscible with Eudragit and Soluplus than with PVP and HPMCAS, and that PVP was more miscible with HPMCAS than Eudragit and Soluplus. This led to different configurations of phase separation in the placebo and drug-loaded fibres. The *in vitro* drug release data confirmed that the use of PVP-Eudragit retained the dissolution enhancement of the PVP formulation, whereas PVP-Soluplus reduced the drug release rate in comparison to FF-PVP formulations. The moisture sorption results confirmed that moisture uptake by the polymer blends was reduced, but formulation deformation occurred to phase-separated blend formulations. The data revealed the importance of miscibility and phase separation in understanding the physical stability of the ES fibre mats. The findings provide insight into the design of formulations that can provide dissolution enhancement balanced with improved storage stability.

**Keywords:** Electrospinning; solid dispersion; polymer blends; poorly soluble drugs; dissolution enhancement; moisture uptake kinetics

## 1. Introduction

Solid dispersions are an effective formulation approach for improving the dissolution, and subsequently the bioavailability of orally delivered, poorly water-soluble drugs [1, 2]. Using electrospinning (ES) to produce micro to nano-size water-soluble polymer fibre based solid dispersion formulations has recently attracted an increasing amount of research attention [3-9]. These fibres form three-dimensional porous matrices that have a great advantage in that their large surface area to volume (SA/V) ratio can provide significant dissolution enhancement of poorly water-soluble drugs [5, 6, 10-12]. One of the intrinsic practical drawbacks of such a high SA/V ratio however is that it can enable increased moisture uptake in the ES fibre formulations, in particular when hydrophilic/hygroscopic polymers, such as PVP, are used. The storage instability of electrospun PVP solid dispersions have been confirmed in the literature [13-17]. These irreversible changes in the formulations as a result of the sorption of moisture typically reduce their dissolution rate significantly [18-21]. Therefore, formulation strategies that can minimise moisture uptake and improve the long-term shelf-life stability of these drug-loaded ES fibres are vitally important for translating their advantages into clinically useful products, but thus far have had limited attention in the literature. Moreover, there is also still a lack of fundamental understanding of the role of the phase separation behaviour in polymer blend formulations on moisture uptake of formulations [13, 14].

Previously the use of polymer blends has been proposed to improve the performance of solid dispersion-based formulations [22, 23]. In the context of this study, the rationale for using polymer blends was to primarily reduce sorption of moisture by the PVP-based formulation for oral delivery of poorly soluble drugs with the intention to improve the storage stability of the formulations whilst still maintaining the dissolution enhancement. Fenofibrate (FF) is a useful model drug to test this as it has a high propensity to recrystallize in a solid dispersion matrix

[24]. This study investigated the use of polymer blends of PVP (K90) with a range of polymers, including dimethyl-aminoethyl methacrylate (Eudragit E<sup>®</sup>), polyvinyl caprolactam-polyvinyl acetate-polyethylene glycol graft copolymer (Soluplus<sup>®</sup>) and hypromellose acetate succinate (HPMCAS). The rationale of selecting these polymers is that they all have lower moisture sorption tendencies than PVP and have the potential to reduce the overall moisture uptake and improve the physical stability of the ES fibre-based solid dispersions. The miscibility study in combination with the detailed moisture sorption kinetic measurements and physical stability study were conducted in order to investigate the possible roles of miscibility and phase separation on the performance of ES formulations. This should provide new insights into the underpinning mechanisms of moisture sorption in polymer blend fibre formulations and new practical strategies to overcome the destabilisation of ES solid dispersions caused by moisture uptake.

## **2. Materials and Methods**

### ***2.1 Materials***

The crystalline fenofibrate (FF) polymorph I used in this study was supplied by Merck Serono (Darmstadt, Germany). Kollidon<sup>®</sup> 90 F (PVP-K90), with an approximate molecular weight of 1,250,000 g/mol, was provided by BASF (Ludwigshafen, Germany). The dimethyl-aminoethyl methacrylate (Eudragit<sup>®</sup> E), approximate molecular weight of 47,000 g/mol, was donated by Evonik Industries (Darmstadt, Germany). The polyvinyl caprolactam–polyvinyl acetate-polyethylene glycol graft copolymer (Soluplus), approximate molecular weight of 118,000 g/mol, was provided by BASF (Ludwigshafen, Germany). Hypromellose acetate succinate (HPMCAS), with an average molecular weight of around 17,000-20,000 g/mol was supplied by Shin-Etsu Chemical Co Ltd. (Niigata, Japan). Dichloromethane and ethanol of reagent grade were purchased from Sigma-Aldrich.

## ***2.2 Electrospun solid dispersion fibres preparation***

All sample solutions (placebo and drug-loaded) were prepared with a total solid content of 10 % (w/v). The polymer to drug ratios for all formulations were 3:1 (w/w). The drug was added into individual polymer solutions (PVP, HPMCAS, Eudragit E and Soluplus) or blended polymer solutions (at a ratio of polymers of 1:1 of PVP: HPMCAS, PVP: Eudragit E and PVP: Soluplus) in a 7:3 ethanol: DCM solvent. These were stirred until clear solutions were obtained. A custom-made electrospinning apparatus was used to prepare the electrospun fibres. The stock solution was fed from a plastic syringe into the apparatus at 1.5 ml/hr using a syringe pump (Cole-Parmer, UK) through a 18 gauge blunt-end needle connected to a high voltage of 15 kV supplied by an ES40P-20W high voltage power supply (Gamma High Voltage Research Inc., Ormond Beach, FL, USA). A custom-made drum collector (with 12 cm in diameter and 30 cm in length) was used to collect the electrospun fibres at 500 RPM. The needle raster remained at a static position during the electrospinning process. The distance between the spinnerette and the collector was set at 15 cm. The electrospinning was conducted under ambient humidity at room temperature (temperature 22 +/- 2C °C and 45-55% relative humidity (RH)) for approximately 3 hours for all formulations. The samples were stored in either 0% RH/RT (RT in this study was set at 22 +/- 2C °C and 0% RH was maintained using P<sub>2</sub>O<sub>5</sub> as a desiccant) for 6 months or 75% RH/RT (75% RH was created and maintained using supersaturated NaCl solution) for 24 hours.

## ***2.3 Film casting preparation***

The same solutions used for electrospinning of PVP and PVP-blend formulations were used to cast the films. One (1) ml of the stock solution was poured into a stainless-steel micrometre adjustable film applicator with adjustable blade gap from 0 to 8 mm with 10 µm increments (TQC Sheen, Leominster, UK) with 100 mm width onto a Teflon plate. A casting gap of 50 µm

was used to obtain a smooth flat film. The films were left in a fume hood for 24 h to allow the organic solvent to completely evaporate.

## ***2.4 Physicochemical characterisation***

### ***2.4.1 Differential scanning calorimetry (DSC)***

A Q-2000 (TA Instruments, Newcastle, DE, USA) was used to perform DSC and modulated temperature DSC (MTDSC) experiments in this study. The T-zero calibration was used to calibrate the baseline. *n*-Octadecane, indium, and tin purchased from Sigma Aldrich were used for temperature calibration. Heat capacity for the MTDSC experiment was calibrated across a temperature range of -60 to 200 °C. A constant nitrogen purge at 50 mL/min was applied during all experiments. A heating rate of 2 °C/min was used for both standard and MTDSC (for MTDSC, a modulation amplitude of  $\pm 1$  °C and a period of 60 s) was used. TA standard aluminium crimped pans and a sample weight between 3-5 mg were used. Each formulation was tested in triplicate.

### ***2.4.2 Attenuated total reflectance Fourier transform infrared spectroscopy (ATR-FTIR)***

An IFS 66/S spectrometer (Bruker Optics Ltd., Coventry, UK) equipped with a Golden Gate heated top plate attenuated total reflectance accessory (Specac Ltd., Orpington, UK) was used to perform the IR spectroscopic studies. A few milligrams of raw materials, crystalline FF, amorphous FF and electrospun fibrous formulations were placed on the diamond crystal of the ATR accessory. Amorphous FF was obtained from the melt of the crystalline FF on the Golden Gate heated top plate ATR accessory at 100 °C. After melting, the molten FF was allowed to cool to room temperature and the spectrum was acquired. Each sample was scanned 32 times between 4000 and 550  $\text{cm}^{-1}$  at a resolution of 2.0  $\text{cm}^{-1}$ . All samples were examined in triplicate.

OPUS software version 6.5 (Specac Ltd., Orpington, UK) was used to analyse ATR-FTIR spectra.

#### ***2.4.3 Power X-ray diffraction (PXRD)***

A Thermo-ARL X'tra diffraction (Ecublens, Switzerland) was used to perform PXRD experiments at ambient temperature and humidity in Bragg-Brentano geometry. The crystalline samples were gently crushed with a mortar and a pestle to avoid the preferred orientation effect. The crushed powders were transferred to a sample holder. Physical mixtures of drug and polymer were homogeneously blended in a mortar before being transferred to the sample holders. The electrospun fibres samples were cut into small pieces prior to being packed onto the sample holders. A Cu  $K\alpha_1$  radiation source was used with 45 kV voltage and a current of 40 mA. The angular range was from 5° to 50° ( $2\theta$ ) with a step size of 0.01° and one second per step.

#### ***2.4.4 Scanning electron microscopy (SEM)***

A JEOL 5900 LV (Tokyo, Japan) scanning electron microscope with a secondary-electron detector and a backscattered electron detector was used to examine the morphology of the electrospun fibres. A small piece of the fibrous mat was attached to a sample stub and sputter coated with Au/Pd before imaging. The acceleration voltage was fixed at 20 kV.

#### ***2.5 In vitro drug release study***

All *in vitro* drug release experiments were performed using the British Pharmacopoeial paddle method with 50 rpm paddle rotation speed at  $37\pm 0.5$  °C and with 500 ml of HCl dissolution medium (pH 1.2). Sodium lauryl sulphate was added to the dissolution medium for each vessel to give a concentration of 0.5 % (w/v) to maintain sink conditions for FF. Pieces

of the electrospun fibre mats that contained the equivalent of 10 mg FF were used for the release experiments. To prevent the ES mats floating on the surface of the dissolution media, the mats were attached to a metal paperclip which was used as a 'sinker' to ensure the mats were completely immersed. At predetermined time intervals (at 1, 3, 5, 7, 10, 20, 30, 60, 90, and 120 minutes), 5 ml of media from each vessel were sampled and filtered through 0.45 µm filters (Minisart Sartorius, Goettingen, Germany) and diluted with 5 ml of ethanol. All dissolution tests were performed under sink conditions. The FF content in each sample was measured with a UV spectrometer (Perkin-Elmer Lambda XLS, USA) at 290 nm. The calibration curve of FF was prepared using pH 1.2 HCl: ethanol (1:1 v/v) media within the FF concentration between 5 to 20 µg/ml. The  $R^2$  of the calibration curve was 0.9998. All measurements were performed in triplicate. The kinetic model fitting was performed using OriginPro 8.0 software (OriginLab Corporation, Northampton, USA).

## ***2.6 Moisture sorption***

A Q-5000 SA DVS (TA Instruments, Newcastle, DE, USA) was used to perform dynamic vapour sorption (DVS) experiments. The samples were freshly prepared and were cut into small pieces. Approximately 8-10 mg of the samples were placed into a quartz pan. All samples were dried under 0% RH for 100 minutes before starting the sorption isotherm/isohumic experiments. During the experiments, the sample chamber was sealed shut and a dry nitrogen purge through a water reservoir was used to control the experimental humidity. For the sorption isotherm experiments, the samples were held at a specific RH in the range 10% to 90% RH (with 10% RH increment increases) for at least 300 minutes at each humidity (with the incremental increase criteria being fluctuations in weight that were less than 0.05% over 10 minutes).

For the kinetic study, the fibre samples were incubated at 75% RH for 400 minutes. Curve fitting of the data was carried out using TableCurve 2D version 5.01 (Systat Software Inc., Chicago, USA) and Qti plot (Iondev SRL, Bucharest, Romania).

### ***2.7 Theoretical $T_g$ calculation using Gordon-Taylor (GT) equation***

The modified GT equation was used to estimate the  $T_g$  of ternary dispersions [25]. The theoretical  $T_g$  values of the FF loaded polymer blend solid dispersions were calculated by this approach using the experimentally measured  $T_g$  of each individual material. The  $T_g$  values of the amorphous FF, PVP, HPMCAS, Eudragit E and Soluplus were  $-20\pm 0.5$ ,  $176.4\pm 2.0$ ,  $122.0\pm 2.2$ ,  $55.8\pm 0.5$ , and  $77.0\pm 0.8$  °C, respectively. Eq. 1 is the adapted GT equation for the ternary system, and  $K$  can be calculated based on the Couchman-Karasz model [26], which was slightly modified to obtain  $K_1$  and  $K_2$ , as seen in the Eq. 2.

$$T_g = \frac{W_1 T_{g1} + K_1 W_2 T_{g2} + K_2 W_3 T_{g3}}{W_1 + K_1 W_2 + K_2 W_3} \quad \text{Eq. 1}$$

$$K_1 \approx \frac{\Delta C_{p2}}{\Delta C_{p1}} \quad \text{and} \quad K_2 \approx \frac{\Delta C_{p3}}{\Delta C_{p1}} \quad \text{Eq. 2}$$

where  $W_1$ ,  $W_2$  and  $W_3$  are the weight fractions of FF, PVP and HPMCAS, Soluplus or Eudragit E;  $T_{g1}$ ,  $T_{g2}$  and  $T_{g3}$  are the  $T_g$  values of amorphous FF, PVP and HPMCAS, Soluplus or Eudragit E; and  $\Delta C_{p1}$ ,  $\Delta C_{p2}$  and  $\Delta C_{p3}$  are the heat capacity changes of FF, PVP and HPMCAS, Soluplus or Eudragit E.

## **3. Results and discussion**

### ***3.1 Drug-polymer and polymer-polymer miscibility study***

Solubility parameters are often used in the literature to estimate the miscibility between pharmaceutical materials [23, 27]. Although this estimation may not be practically accurate, it can be used as a starting point for comparative purposes. An estimation based on the theoretical calculation of the solubility parameters (detailed in the **Supplementary Materials Table S1**)

suggested that PVP should be miscible with HPMCAS, Soluplus and Eudragit [22, 23]. However, such theoretical predictions often deviate from the experimental results [28]. Therefore at 1:1 w/w ratio, the miscibilities of the polymer pairs were examined using experimentally measured  $T_g$  values by MTDSC on the placebo ES fibres. The results revealed different degrees of miscibility between PVP and the three pairing polymers. As seen in **Table 1**, freshly prepared PVP-HPMCAS placebo fibres showed a single  $T_g$  at  $152.4 \pm 1.0$  °C, indicating the formation of a single-phase (**Figure 1a**). This  $T_g$  is very close to the predicted  $T_g$  of the two polymers using the Gordon-Taylor (G-T) equation indicating their good miscibility [29,30]. All detailed calculation of G-T  $T_g$ s can be found in the **Supplementary Materials (Table S2)**. In contrast, two  $T_g$ s were observed for the freshly prepared PVP-Soluplus and PVP-Eudragit placebo fibres indicating a certain degree of phase separation. PVP-Soluplus shows a partially miscible phase (with a  $T_g$  of  $91.9 \pm 1.9$  °C) and a PVP-rich phase (with a  $T_g$  of  $175.7 \pm 0.9$  °C). According to the G-T calculation, the phase with a  $T_g$  of  $91.9$  °C contains approximately 74:26 (w/w) of Soluplus: PVP ratio. The two  $T_g$ s of PVP-Eudragit placebo fibres at  $48.6 \pm 1.8$  and  $175.3 \pm 2.4$  °C are close to the  $T_g$ s of each polymer suggesting poor miscibility and almost complete phase separation.

**Table 1. Summary of the experimentally measured  $T_g$  of the binary and ternary dispersions.**

<b>ES placebo polymer blend fibres</b>				
	<b>PVP-HPMCAS</b>	<b>PVP-Soluplus</b>	<b>PVP-Eudragit</b>	
<b><math>T_g</math> (°C)</b>	$152.4 \pm 1.0$	$91.9 \pm 1.9$ $175.7 \pm 0.9$	$48.6 \pm 1.8$	$175.3 \pm 2.4$
<b>Casted FF-single polymer films</b>				
	<b>FF-PVP</b>	<b>FF-HPMCAS</b>	<b>FF-Soluplus</b>	<b>FF-Eudragit</b>
<b><math>T_g</math> (°C)</b>	$103 \pm 3.2$ (with observed drug melting)	$54.3 \pm 1.3$ (with observed drug melting)	$21.2 \pm 0.7$	$4.2 \pm 0.9$

Casted FF-polymer blend films			
	FF-PVP-HPMCAS	FF-PVP-Soluplus	FF-PVP-Eudragit
T <sub>g</sub> (°C)	Not measurable (potentially superimposed with FF melting)	5.9 ± 1.1 116.8±1.7	-6.5 ±1.4 117.5±0.3

The miscibility of FF with each individual polymer was also examined. As FF could not be directly electrospun with Soluplus, HPMCAS or Eudragit E, individually, FF was cast into solid dispersions films with a polymer to drug ratio of 75:25 (w/w). As seen in **Table 1** and **Figure 1b**, the FF-PVP and FF-HPMCAS films showed a small crystalline FF melting at 80 °C, and the T<sub>g</sub>s can be observed at 103±3.2 for FF-PVP and 54.3±1.3 °C for FF-HPMCAS, respectively. This result indicates that at 75:25 polymer to drug ratio FF is supersaturated in PVP and HPMCAS which led to the rapid recrystallisation of the FF in the freshly prepared samples. The measured T<sub>g</sub> of the FF-PVP is higher than the predicted T<sub>g</sub> (approximately 96.4 °C) by G-T calculation. This is due to rapid and significant drug recrystallisation, confirmed by the SEM images of the films seen in **Figure 1c**, which reduced the drug content retained as a molecular dispersion in PVP. The measured T<sub>g</sub> of the FF-HPMCAS film is lower than the predicted G-T T<sub>g</sub> (approximately 65.4 °C). Such negative deviations have been previously suggested to be caused by stronger drug-drug interactions than drug-polymer interactions [30]. This may explain the rapid drug recrystallisation in FF-HPMCAS. The FF-Eudragit E and FF-Soluplus cast films demonstrate single T<sub>g</sub>s at 4.2±0.9 °C and 21.2±0.7 °C, respectively, without any detectable crystalline FF melting. These results confirmed that FF has a higher solubility in Eudragit E and Soluplus than in PVP and HPMCAS.

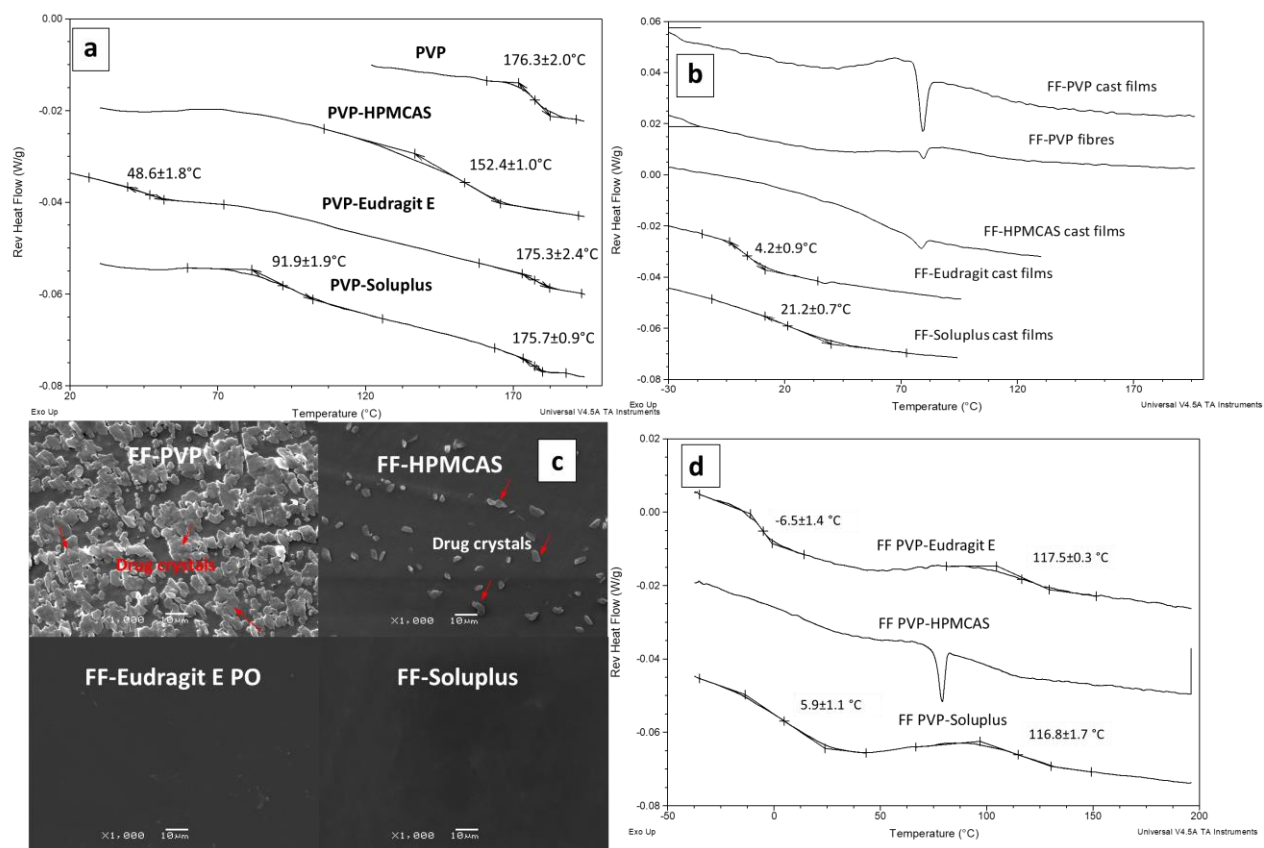


**Figure 1** MTDSC results of freshly prepared (a) placebo ES fibres; (b) binary FF-single polymer cast films; (c) SEM images of the binary cast films; (d) ternary FF-polymer blends cast films.

The multi-component nature of the FF-polymer blend systems made assessment of the miscibility of FF with the polymer blends challenging. Crystalline drug melting was detected for the cast FF-PVP-HPMCAS film indicating poor miscibility of FF in the PVP-HPMCAS. No  $T_g$  was observed; this might have been obscured by the drug melting peak. Double  $T_g$ s were observed in the cast films FF-PVP-Eudragit and FF-PVP-Soluplus films (**Table 1, Figure 1d**) and are much lower than those of the respective placebo formulations. The shifts of the  $T_g$ s to lower temperatures are likely to be due to FF being molecularly incorporated and plasticising each polymer phase.

From the miscibility estimations, it is clear that FF has relatively good miscibility with Eudragit E and Soluplus, but poor miscibility with HPMCAS and PVP. This led to improved miscibility of FF in the polymer blends of PVP-Eudragit and PVP-Soluplus than PVP-HPMCAS. However, of the polymer blends themselves, PVP-HPMCAS exhibited better miscibility with a single phase formed at 1:1 (w/w), whereas, PVP-Eudragit and PVP-Soluplus formed two-phase dispersions with a PVP-rich phase and Eudragit or Soluplus-rich phase. Although FF could be molecularly dispersed in both polymer phases in the phase separated polymer blends, because of its higher miscibility with Eudragit and Soluplus, it is likely that the amount of FF dispersed in the Eudragit/Soluplus phases was higher than that in the PVP phases in the case of FF-PVP-Eudragit and FF-PVP-Soluplus formulations. The risk of high moisture sorption and drug recrystallisation is likely to be high in the PVP-rich phase.

### ***3.2 Characterisation of FF-polymer blend ES fibres***

The placebo PVP fibres were smooth with an average diameter of  $0.75 \pm 0.24 \mu\text{m}$ . The solutions of the placebo mono-polymer of Eudragit E and Soluplus at 10% (w/v) solid content concentration were not electrospinnable and HPMCAS formed beaded fibres (**Figure 2**). Blending with PVP in the ratio of 1:1 (w/w) significantly enhanced the electrospinning processibility of these polymers. Smooth cylindrical fibres were formed with an average diameter of  $1.29 \pm 0.41$ ,  $0.82 \pm 0.22$  and  $1.07 \pm 0.25 \mu\text{m}$  for PVP-HPMCAS, PVP-Eudragit E and PVP-Soluplus, respectively. The drug loaded fibres had diameters of  $0.51 \pm 0.02$ ,  $0.77 \pm 0.17$ ,  $1.03 \pm 0.39$  and  $0.77 \pm 0.16 \mu\text{m}$  for FF-PVP, FF-PVP-Eudragit E, FF-PVP-HPMCAS and FF-PVP-Soluplus, respectively (**Figure 2**). In general, the fibre diameters of the drug-loaded fibres were smaller than the placebo fibres. This effect may be attributed to reduced viscosity of the drug containing ES solutions which had a total polymer content of 7.5% (with 2.5% drug) in comparison to the 10% polymer concentration placebo solutions.

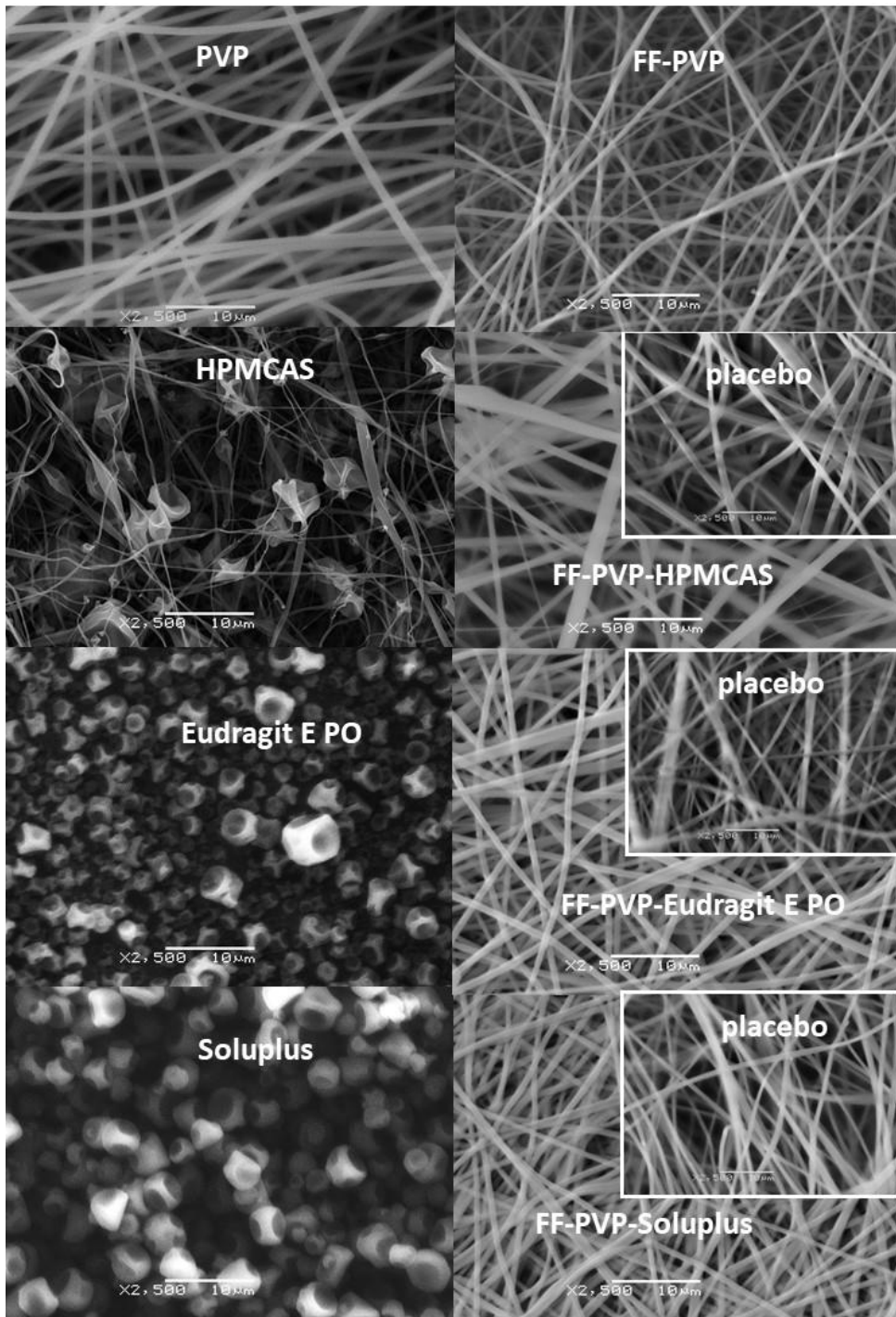


**Figure 2** SEM images of the freshly prepared placebo and drug-loaded ES formulations.

The scale bars in all SEM images represent 10 μm.

The physical state of FF in the freshly prepared ES fibre solid dispersions was further studied using DSC, ATR-FTIR spectroscopy, and PXRD. It is clear from the DSC results that

a low level of drug melting at approximately 80 °C can be detected in FF-PVP-HPMCAS (**Figure 3a**). The recrystallisation of FF could be attributed to the high drug loading used in this study (25% w/w) which may have reached the saturated solubility of FF in the polymer. No drug melting was detected in FF-PVP-Eudragit and FF-PVP-Soluplus. Due to the noisy baseline, no clear  $T_g$  was detected by DSC, and even with the use of MTDSC, no  $T_g$  was observed in the reversing signals of the freshly prepared dispersions (see **Figure S1** in **Supplementary Materials**). A small diffraction peak also can be seen in the PXRD data of FF-PVP-HPMCAS (**Figure 3b**) indicating the presence of a small quantity of recrystallised FF. This is likely due to the poor miscibility FF in both PVP and HPMCAS as detected in the miscibility study.

No signature crystalline FF peak was seen in the ATR-FTIR spectra of all ES fibres formulations (**Figure 3**). With comparison to the ATR-FTIR spectrum of amorphous FF (which corresponds with that reported in the literature [31, 32]), no clear shifts in the signature peaks of amorphous FF can be seen in the spectra of the FF-PVP and FF-polymer blend dispersions, indicating no obvious drug-polymer intermolecular interactions which agrees well with the results of the miscibility study (**Figure 3c and d**).

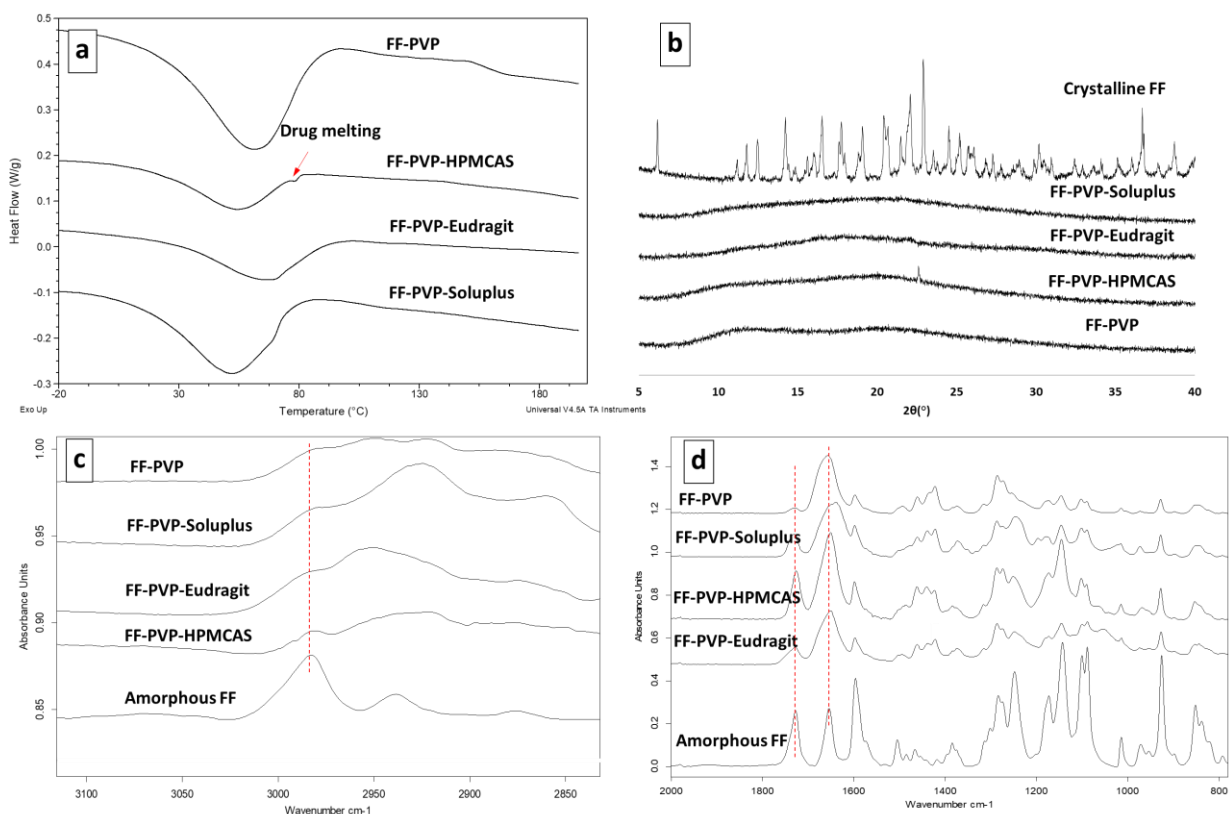


**Figure 3** (a) DSC, partial ATR-FTIR spectra of (b) 3200-2850  $\text{cm}^{-1}$  and (c) 2000-800  $\text{cm}^{-1}$  regions of the FF-loaded polymer blend ES fibres, and (d) PXRD diffraction patterns of the FF-loaded ES fibres and crystalline FF as the reference.

### 3.3 Dissolution of freshly prepared FF-polymer blend ES fibres

As illustrated in **Figure 4**, all of the ES formulations demonstrated significant dissolution enhancement of FF in comparison to the crystalline FF form I powder under sink conditions. PVP is well-known for being used as an ultrafast ES fibrous matrix to improve the solubility of BCS class II drugs such as FF [12, 32-41]. In this study, FF-PVP fibres showed the fastest drug release with over 50% drug release ( $t_{50}$ ) in under 2 minutes. The second fastest drug release was obtained from FF-PVP-Eudragit E fibres owing to the highly soluble nature of Eudragit E under acidic pH. The poorer solubility of Soluplus and the insoluble nature of HPMCAS at acidic pH led to the slower drug release from FF-PVP-Soluplus ( $t_{50}$  of 23 minutes) and FF-PVP-HPMCAS ( $t_{50}$  of 80 minutes) [11]. pH 1.2 HCl was used as the media for this

study, but the FF-PVP-HPMCAS formulations may have faster dissolution in intestinal pH in which HPMCAS becomes more soluble. These results demonstrate that a range of the drug release profiles can be achieved by blending polymers of different dissolution rate/solubility in the media.

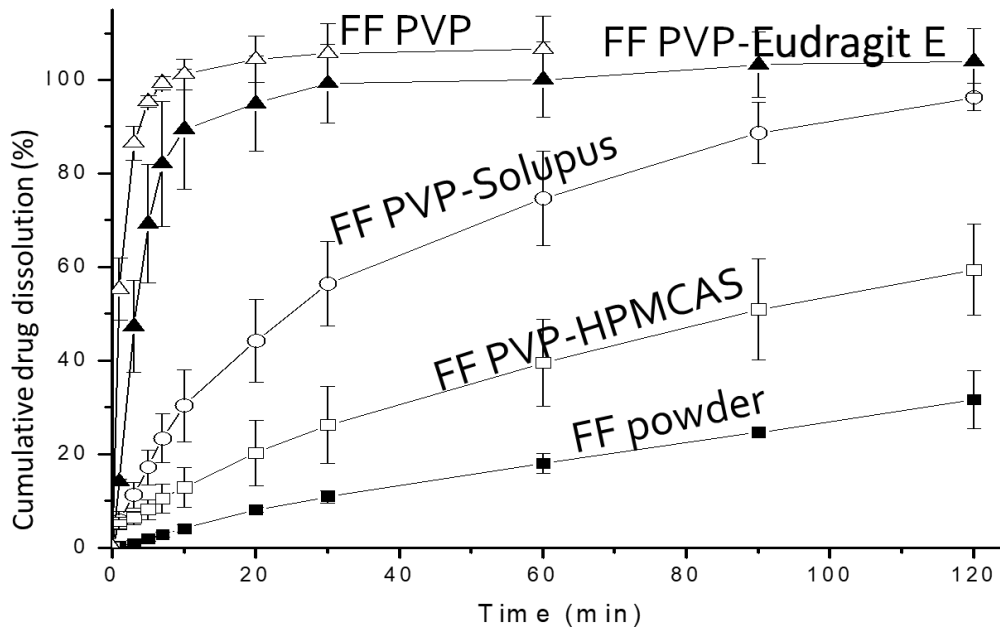


**Figure 4** *In vitro* drug release profiles of FF loaded fibres in pH 1.2 media with 0.5% w/v SLS.

### 3.4 Kinetics of moisture sorption of ES fibres

The common polymer used in this study, PVP, is a highly hygroscopic polymer. Therefore the formulations prepared using it carry a high risk of rapid moisture uptake which could induce drug recrystallisation and lead to undesirable physical instability. A fuller understanding of the moisture uptake kinetics of the fibres would allow a better prediction of their physical stability against high humidity. Therefore, sorption isotherm and isohumic kinetic experiments were performed. The sorption isotherm enables examination of the equilibrium moisture uptake; whereas the isohumic experiments carried out at 75% RH/RT, the relative humidity in standard

accelerated stress conditions and the conditions used for the storage stability tests [43], allow examination of the moisture sorption kinetics.

#### *3.4.1 Sorption isotherm*

The sorption isotherm experiments were performed at RT (22+/-2 °C) for the placebo and FF-loaded ES fibres. The moisture uptakes of these fibres are reported as the ratios of the weight of water absorbed to the polymers dry weight ( $G_{\text{water}}/G_{\text{polymer}}$ ), as indicated by the Y-axis of **Figure 5**. In terms of the amount of moisture uptake, the PVP based fibres showed greatest moisture sorption capability. It is clear that the blending of PVP with the non-hygroscopic polymers reduced the moisture uptake capacity by approximately 40-50%. Eudragit and HPMCAS were more effective in reducing in moisture uptake than Soluplus. This could be attributed to the low level of intrinsic moisture sorption of pure Eudragit E and HPMCAS, as seen in **Figure 6**. This is true for both placebo and drug loaded fibres.

FF, being poorly soluble, would be expected to reduce the hydrophilicity of the fiber mats, but the plots of water uptake for the placebo and FF loaded ES fibres were very similar. As no drug-polymer interaction was detected in the characterisation study, it is reasonable to hypothesise that the amorphous drug was encapsulated by the polymer phases and acted as inert diluent in the mat which did not affect the moisture sorption behaviour of the polymers.

Although the trend is clear, using kinetic analysis of the sorption data of the polymer blend fibres to understand the underpinning moisture uptake mechanism is highly complex [44]. The sorption isotherm data (the equilibrium moisture contents from 10% to 90% RH) of the ES fibres were fitted to the Guggenheim-Anderson-de Boer (GAB) model. The GAB model is a versatile mathematical model to describe non-linear moisture sorption behaviour in foods and

pharmaceutical materials. It is an isothermal type II (sigmoidal shape) model [45-47] and can be expressed as:

$$M = \frac{M_0 C_G K a_w}{(1 - K a_w)(1 - K a_w + C K a_w)} \quad \text{Eq. 3}$$

where  $M$  is the ratio of the weight of water ( $G_{\text{water}}$ ) taken up to the dry weight of the polymer ( $G_{\text{polymer}}$ ),  $a_w$  is the water activity which is equal to the relative humidity at the equilibrium state,  $M_0$  is the monolayer moisture content,  $C_G$  is Guggenheim constant and  $K$  is the compensating constant for multilayer moisture adsorption. A good fit indicated by a  $R^2$  at or above 0.999 was obtained for both placebo and drug-loaded samples (**Figure 5**). Although the GAB model is used as a tool to compare the shapes of the curves arising from different samples, the parameters generated from the GAB model fitting do not have true physical meanings that describe the sorption process [48]. Therefore, the fitting parameters,  $M_0$ ,  $C_G$ , and  $K$ , are not presented and discussed here, but can be found in **Supplementary Materials Table S3**. Nevertheless, the fact that both placebos and drug-loaded polymer blend formulations exhibited highly similar the GAB fitting and with similar  $G_{\text{water}}/G_{\text{polymer}}$  ratios indicated that the incorporated FF simply acted as inert diluent in the dispersion and did not affect the moisture uptake capability of the polymers.

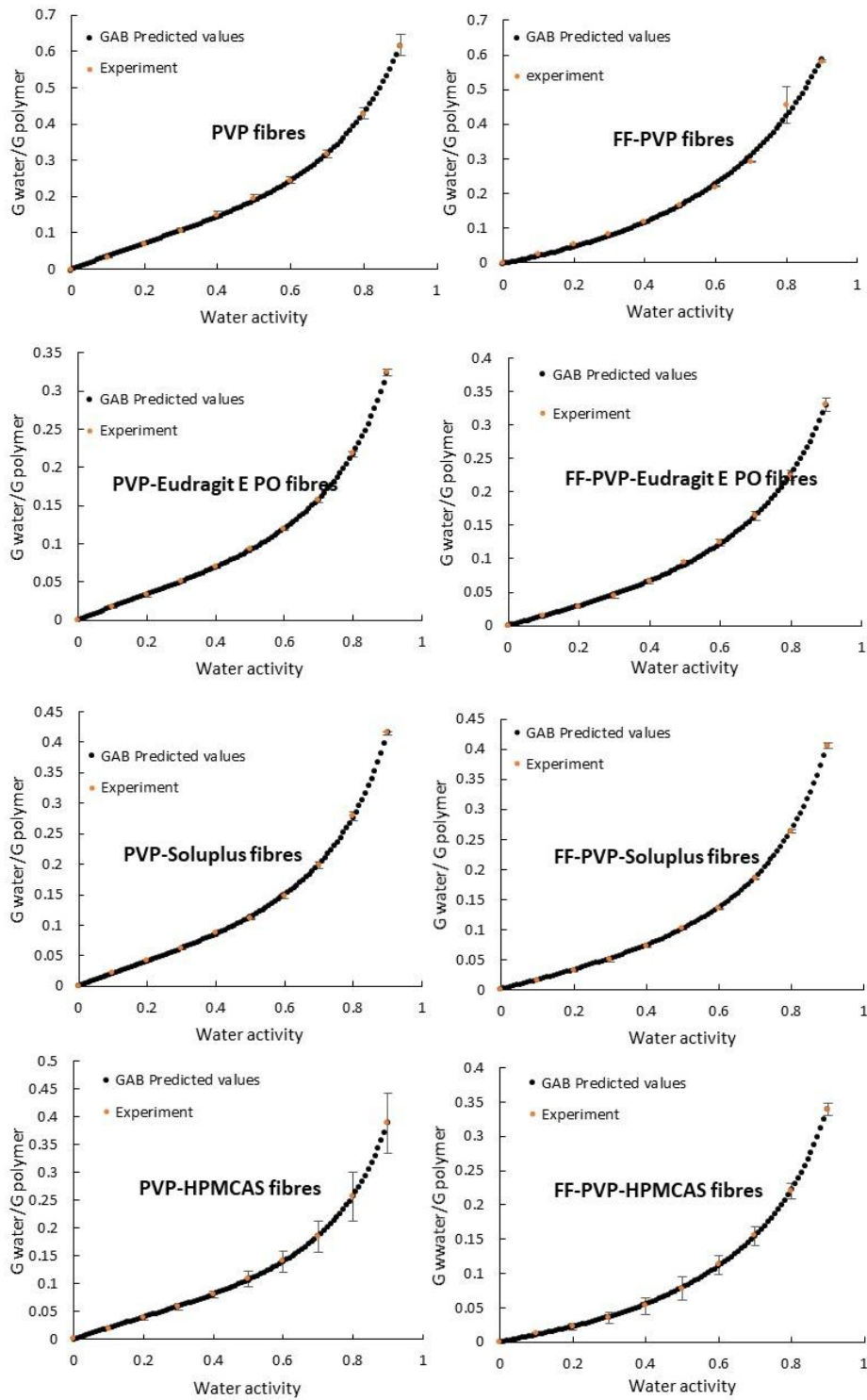


**Figure 5** Sorption isotherms and fitting to GAB model of the placebo and FF-loaded ES fibres.

### 3.4.2 Isohumic sorption kinetics of ES fibres at 75% RH/RT

To further explore the moisture sorption behaviour of the fibres under the humidity that is relevant to real storage conditions of stress testing, isohumic water absorption at 75% RH and room temperature was performed on the raw materials, the placebo ES fibre mats and drug loaded ES fibre mats. Typical results are shown in **Figure 6a** and the full data of all formulations can be found in the **Supplementary Materials Figure S2-S4**. After 300 minutes of isohumic sorption experiment at 75% RH/RT, the samples reached steady-state equilibrium (that is the change in weight of the samples fluctuated by less than 0.2% over the final 100 minutes). As seen in **Figure 6b**, the absolute values of the equilibrium moisture uptake of the drug-loaded samples at the steady-state are less than those for the placebo samples. However, when the results were expressed as moisture uptake per gram of polymer, the results of the drug-loaded samples are very close to the values for the placebo samples (**Figure 6c**). This is consistent with the indication of the GAB fitting results and confirmed that the drug has a little effect on the moisture sorption behaviour of the polymer. This is consistent with the lack of evidence of any drug-polymer interaction.

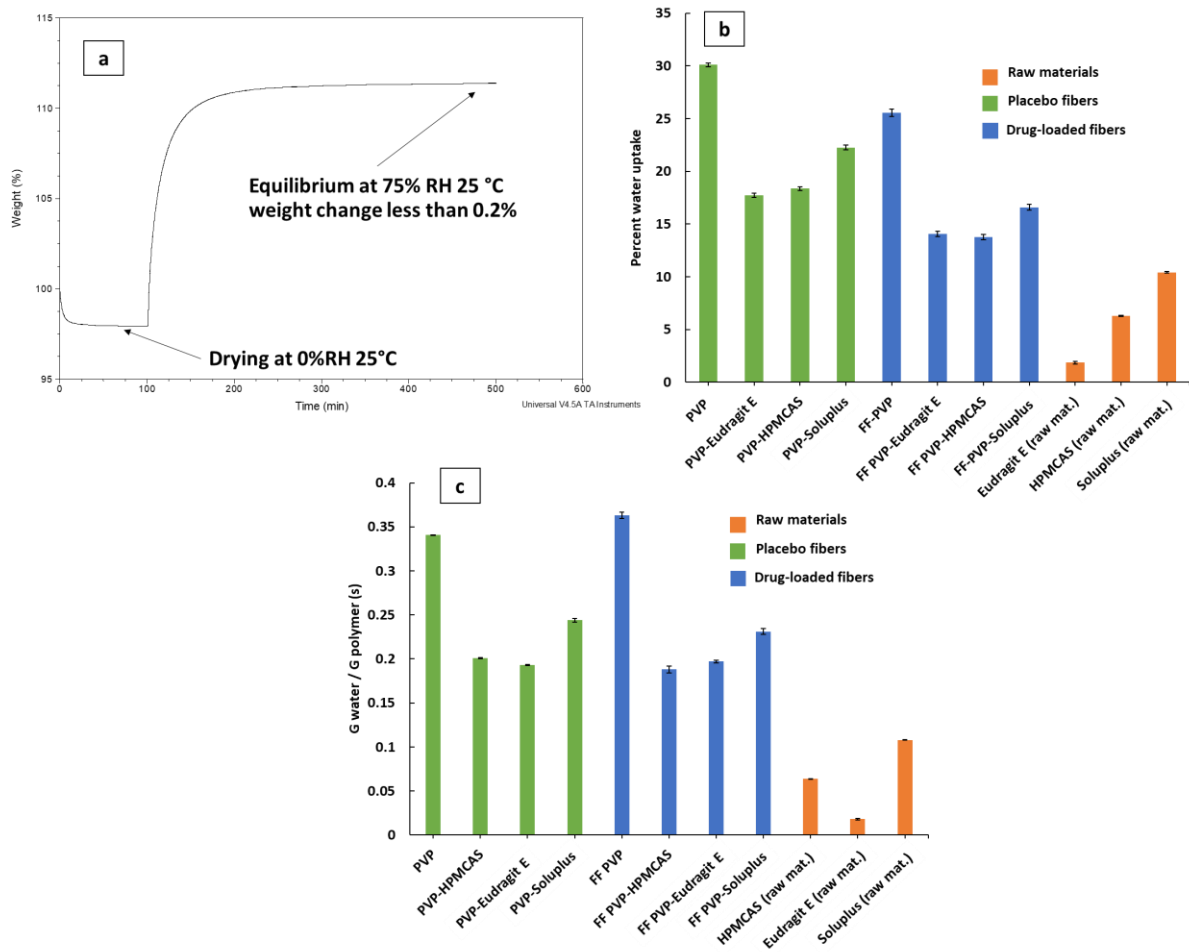


**Figure 6** (a) Typical isohumic sorption DVS curve; (b) absolute equilibrium moisture uptake of the raw materials, placebo and drug loaded solid dispersions; and (c) moisture uptake expressed as  $G_{water}/G_{polymer}$  of the polymer of raw materials, placebo and drug loaded solid dispersion fibres at 75%RH/RT for 400 minutes

As has been shown in the literature previously [48], moisture uptake in polymeric systems is complex and more than one mechanism can be involved. Fitting of the uptake data may be difficult and different models may be appropriate for different parts of the uptake curve [48, 49]. Here attempts were made to fit the isohumic sorption curves using exponential models. A single exponential model did not result in a good fit; thus, double exponential models were used as moisture uptake models taking the form:

$$m_t = m_\infty(1 - (P \exp(-k_1 t) + (1 - P) \exp(-k_2 t))) \quad \text{Eq. 4}$$

$m_\infty$  is of the mass of water taken up per gram of sample at time,  $t=\infty$  and is the inverse of  $A_2$ ,  $k_i$  are the rate constants for processes 1 and 2.  $P$  is the fraction of  $m_\infty$  corresponding to the rate of uptake  $k_1$ . Half-life is defined as the value of  $t$  at which  $\frac{m_t}{m_\infty} = 0.5$ . As an example of the fitting in **Figure 7**, the double exponential model provides a good fit to the whole 400 minutes of the uptake curve. The sorption results of the formulations and the fitting parameters are summarised in **Table 3**.

From the analysis of the fitting parameters, there does not seem to be any correlation of overall rate (as measured by half-life in **Table 3**) with fibre diameter (measured using the SEM images of the fibre with an example seen in **Figure 1**). Thus simple effects of the size of the surface area do not seem to be relevant in this case. The effect of the incorporation of FF generally is to lengthen half-life, as would be expected if the polymer is the main source of water absorption. However, PVP-Eudragit is exceptional in that the presence of drug shortens the half-life. This could be due to phase separation behaviour of the polymers which is discussed later in the stability section.

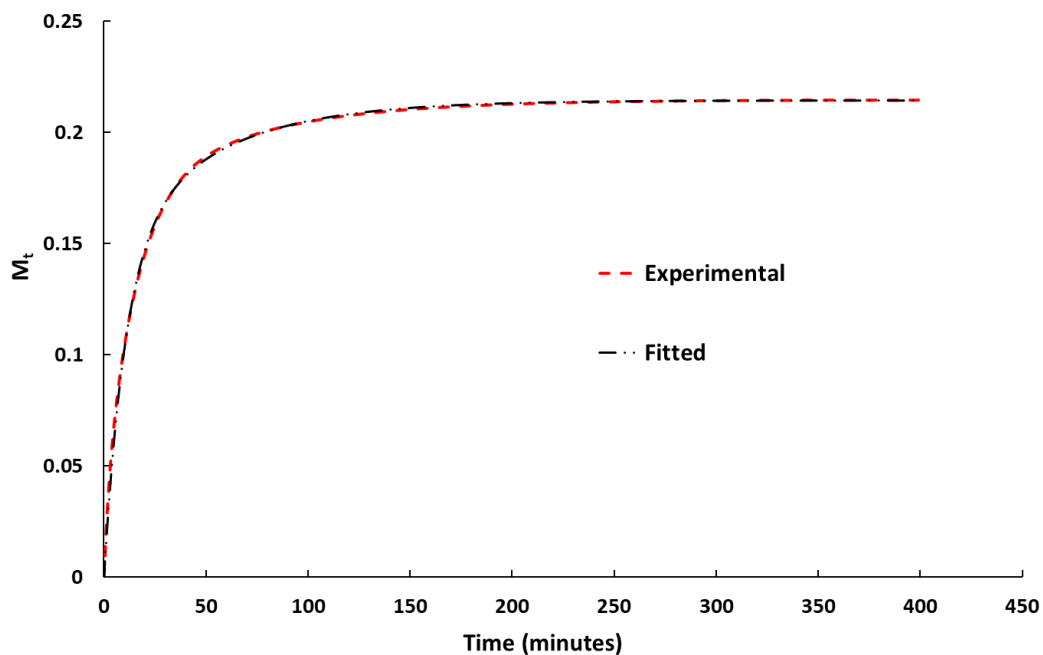


**Figure 7** Examples of the isohumic moisture sorption of FF-PVP ES fibres data with the fit from the double exponential model.  $M_t$  is the mass of moisture sorption per gram of sample which is unitless.

**Table 3.** Experimental data of sorption isotherm and isohumic experiments and fitting parameters to double exponential models of the isohumic results of the ES fibres with the data collected up to 200 minutes. G: water uptake at 75% RH (in terms of weight of water taken up per weight of dry polymer) from the sorption isotherm experiment. K: water uptake at 75% RH (in terms of weight of water taken up per weight of dry polymer) from the isohumic experiments.

Formulation	Experimental data			Isohumic sorption data (double exponential model fitting)					
	G <sup>a</sup>	K <sup>b</sup>	K/G	k <sub>1</sub> <sup>c</sup> (min <sup>-1</sup> )	k <sub>2</sub> <sup>c</sup> (min <sup>-1</sup> )	P <sup>d</sup>	Half life (minute)	m <sub>∞</sub> <sup>b</sup>	m <sub>∞</sub> observed
PVP	0.36	0.341	0.930	0.107	0.021	0.70	9.3	0.341	0.341
PVP-HPMCAS	0.20	0.201	0.960	0.134	0.038	0.44	8.8	0.201	0.201
PVP-Eudragit	0.18	0.193	1.070	0.160	0.036	0.51	8.1	0.192	0.193
PVP-Soluplus	0.22	0.244	1.080	0.159	0.032	0.48	9.1	0.244	0.244
FF-PVP	0.33	0.364	1.090	0.077	0.018	0.67	13.4	0.270	0.273
FF-PVP- HPMCAS	0.18	0.196	1.020	0.129	0.028	0.58	9.5	0.140	0.141
FF-PVP- Eudragit	0.19	0.188	1.042	0.137	0.022	0.76	7.3	0.147	0.147
FF-PVP- Soluplus	0.21	0.231	1.073	0.107	0.015	0.73	9.4	0.172	0.173

a: all fitting errors less than  $1 \times 10^{-3}$

b: all fitting errors less than  $1 \times 10^{-2}$

c: all fitting errors less than  $1 \times 10^{-4}$

d: all fitting errors less than  $1 \times 10^{-2}$

The results indicate that two kinetic processes ( $k_1$  and  $k_2$ ) are taking place, one rapid and the other slower. The rapid process may correspond to moisture uptake with relatively little change to polymer conformation with the slower process involving polymer rearrangement and corresponding morphological changes (as seen in **Figure 8 and 9**) resulting in further moisture uptake. The general goodness of fit of the exponential model implies that the processes are first order. This is not consistent with a diffusional model which would require a fit to an infinite sum of exponential terms. As such, diffusion of water vapour into the fibres cannot be the rate determining step. This is because the fibres have small diameters and so the diffusion process through them is very fast and in effect, they have a homogeneous distribution of water within them at any time. The absorption process then takes on the character of a homogeneous reaction process, the overall time scale of which, is characterised by such factors as polymer reorganisation.

### ***3.5 Physical stability of FF-loaded ES fibres***

Many studies have reported excellent dissolution enhancement of freshly prepared ES formulations, but there is poor understanding on how the high surface area to volume ratio of the ES fibre formulations impacts on their longer-term storage stability. The highly hygroscopic nature of PVP is often a significant factor leading to physical instability on aging for PVP-based solid dispersions [13,14]. In this work, the effects of blending PVP with non-hygroscopic polymers on the physical stability of the fibres were studied by incubating the samples in 75% RH/RT. 75% RH is the standard condition for the accelerated stability study of pharmaceutical products [50]. Thus, we use this particular RH to stress test physical stability which includes drug recrystallisation and structural deformations of the mats.

All placebo and FF-loaded fibre mats were flexible and easy to handle before aging. As in **Figure 8**, aging at 75% RH/RT led to the complete deformation of the placebo and FF-loaded PVP fibre mats. Similar structural deformations (significant shrinkage and increased rigidity) are seen the placebo PVP-Eudragit and PVP-Soluplus based fibre mats after aging. The deformations were significantly worsened by the incorporation of FF. This made in vitro dissolution testing of the aged formulations impossible. On the contrary, the placebo and FF-loaded PVP-HPMCAS based fibre mats exhibited no macroscopic structural deformation.

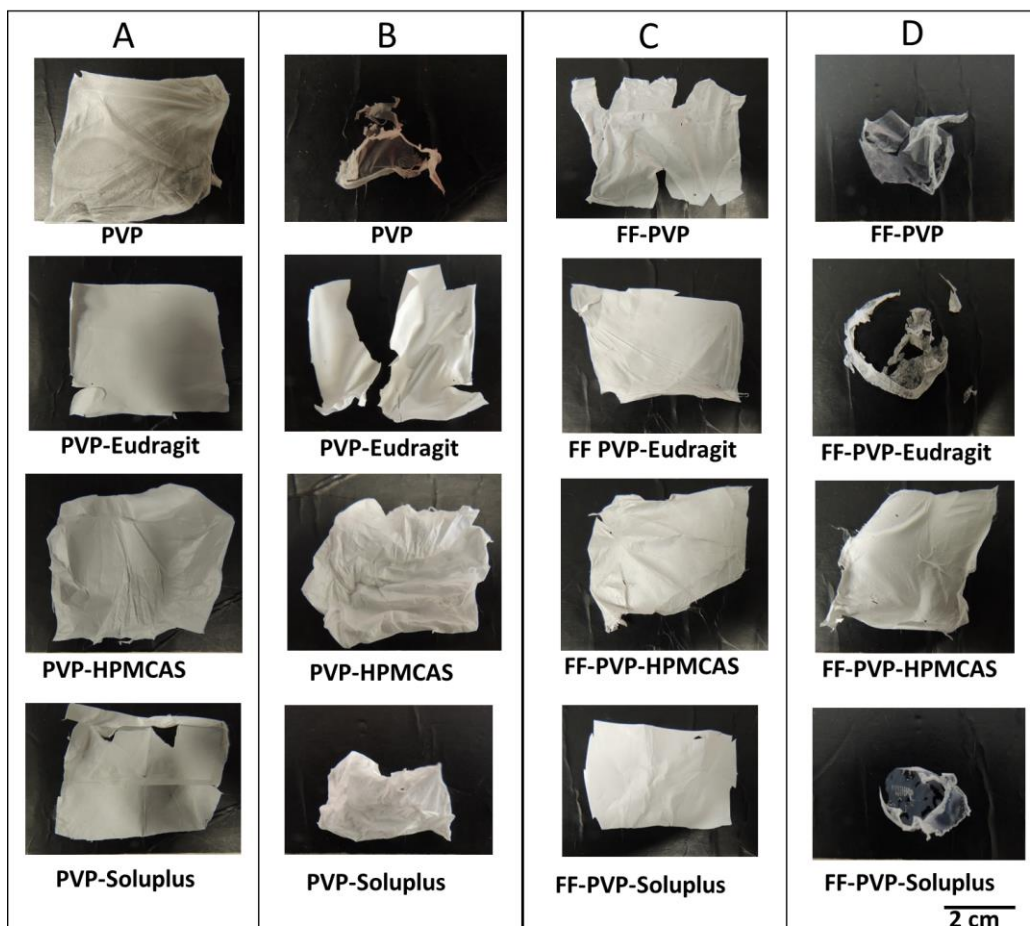


**Figure 8** Appearances of placebo and FF-loaded ES fibres before and after ageing under 75% RH/RT for 24 hours. The placebo ES fibres (A) before and (B) after aging. The FF-loaded ES fibres (C) before and (D) after aging. The scale bar at the bottom right corner is applicable to all images.

The SEM images revealed that for all the placebo fibres a certain degree of swelling and merging between fibres occurred which would reduce the porosity of the film (**Figure 9**). PVP fibres showed the most significant swelling and merging which is likely due to the hygroscopic nature of PVP [51, 52]. Complete loss of the recognizable fibrous morphology and drug crystals can clearly be seen in FF-PVP, FF-PVP-Eudragit E and FF-PVP-Soluplus formulations. PVP-HPMCAS and FF-PVP-HPMCAS fibres show the least morphological changes and only exhibit a mild level of fibre swelling/flattening with less drug crystals than the others. These microscopic changes on the morphologies of the individual fibres could lead to the macroscopic structural deformation for both placebo and FF loaded fibre mats.

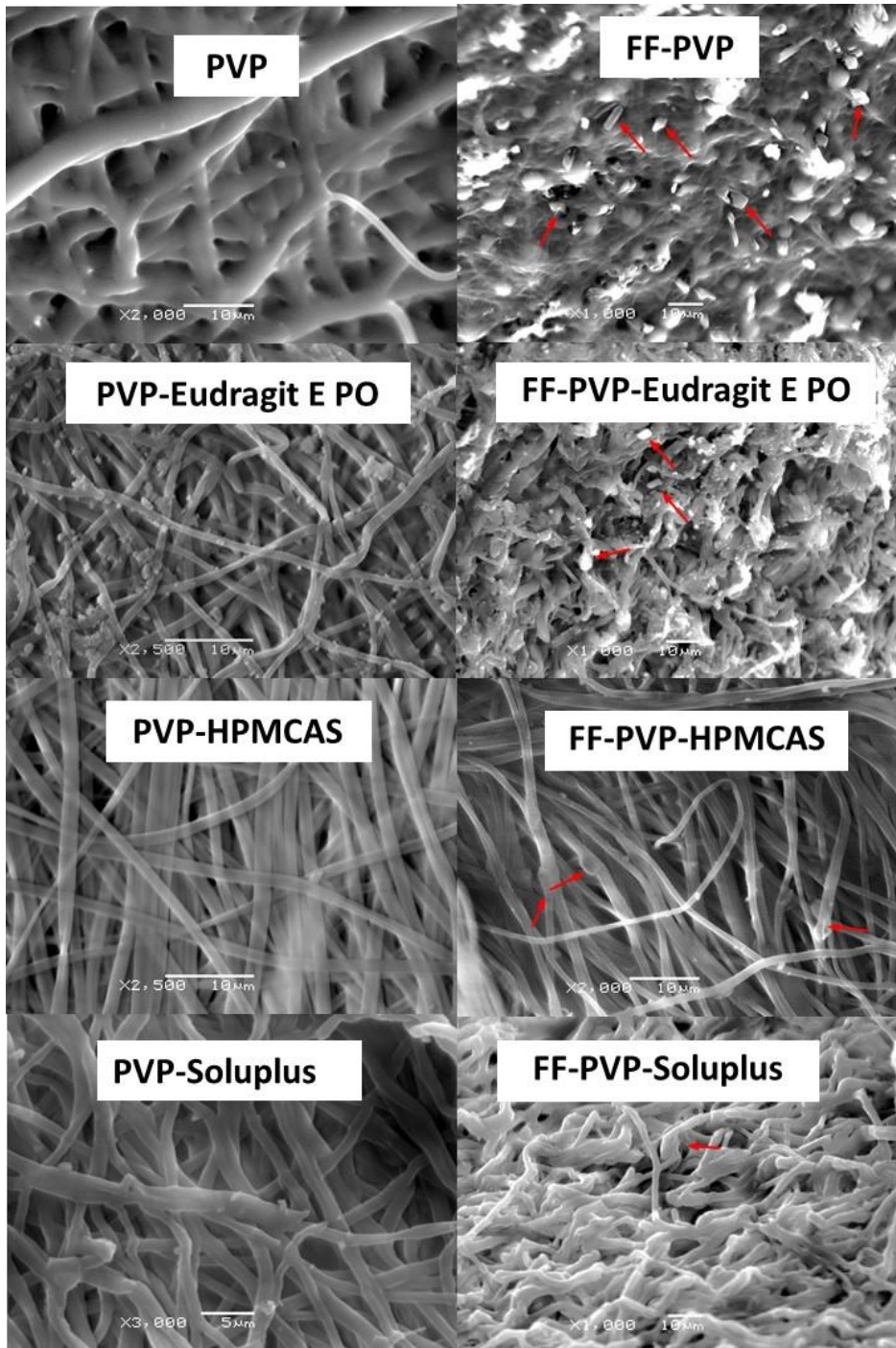


**Figure 9** SEM images of placebo and FF-loaded ES fibres after isohumic sorption experiment under 75% RH/RT in DVS for 400 minutes (red arrows highlight micro crystals of FF on the fibres).

The recrystallization of FF caused by the high humidity storage was further confirmed by DSC and PXRD data. As seen in **Figure 10a**, small FF melting peaks are observed in the DSC results of FF-loaded fibres. The melting enthalpies cannot be clearly measured from the heat

flow signal due to the broad superimposed moisture loss peak but can be used to semi-quantitatively estimate the level of the crystalline content of the drug. FF-PVP-HPMCAS shows the largest melting peak indicating highest amount of recrystallised drug. This agrees well with the PXRD results shown in **Figure 10b**, in which FF-PVP-HPMCAS exhibits the highest peak intensity of the signature diffraction peak of the recrystallised FF at approximately  $22.4^\circ 2\theta$ .

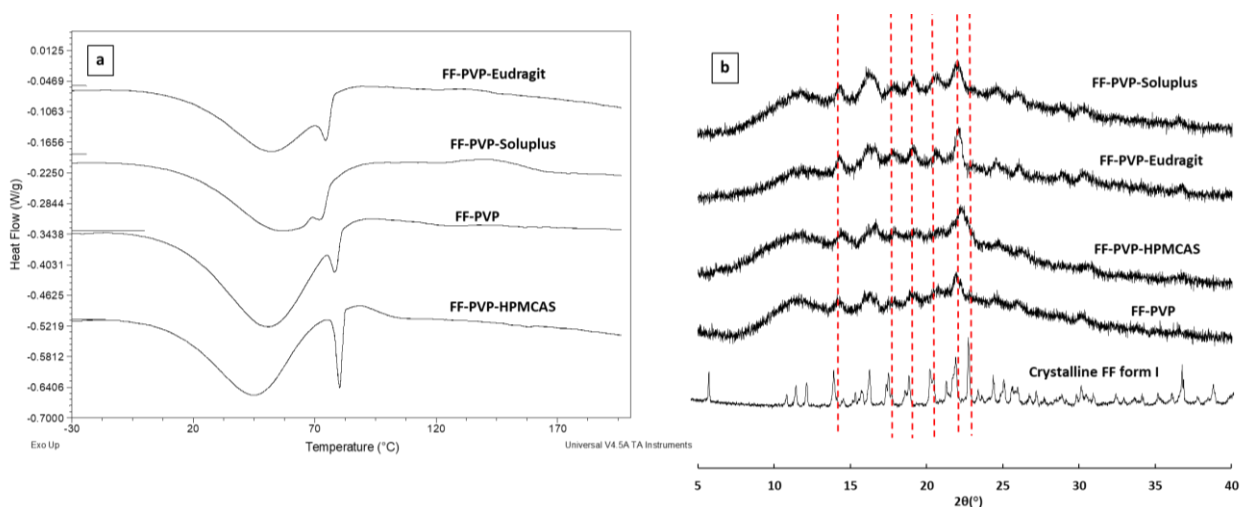


**Figure 10** (a) DSC and (b) the PXRD pattern of FF-loaded ES fibres after being aged in DVS at 75%RH/RT for 400 minutes (the peak intensity of the diffraction patterns of the post-75% RH treatment are magnified 2.5 time in order to highlight the diffractions peaks which would otherwise be difficult to identify)

The storage stability results indicated that HPMCAS can provide the best macroscopic physical integrity protection and minimise the deformation of the fibre mats under high humidity. However, the FF-PVP-HPMCAS fibres displayed the highest level of drug recrystallisation in comparison to the other two polymer-blend formulations. We hypothesise that the phase separated states of these formulations played a key role in this outcome. As illustrated in **Figure 11**, the fresh FF-PVP-HPMCAS is likely to be a single-phase solid dispersion due to the good miscibility between PVP and HPMCAS. FF has poor miscibility

with PVP and HPMCAS, thus the FF loading is likely to approach saturation in the FF-PVP-HPMCAS formulations. Exposure to high humidity consequently led to a high level of drug recrystallisation although single-phase blend of PVP and HPMCAS led to reduced moisture sorption of the fibres sufficiently to prevent deformation. In the cases of FF-PVP-Eudragit and FF-PVP-Soluplus, due to the poor miscibility between PVP and Eudragit/Soluplus, phase separation was expected (as illustrated in **Figure 11**). Because Eudragit and Soluplus have better miscibility with FF than PVP, it is reasonable to hypothesise that a higher amount of drug would distribute in the Eudragit/Soluplus phases instead of PVP phase. The polymer phase separation would not protect PVP from absorbing moisture, thus swelling and physical deformation were seen. However, as less drug was distributed in the PVP phases, lower amounts of the recrystallised drug were detected in FF-PVP-Eudragit and FF-PVP-Soluplus than in FF-PVP-HPMCAS. As the aged FF-PVP-Eudragit exhibited similar level of drug recrystallisation as the aged FF-PVP and similar drug release rates of the fresh samples, similar dissolution performance of the aged FF-PVP-Eudragit and aged FF-PVP are likely to be achieved, but the polymer blend formulation led to reduced moisture sorption.

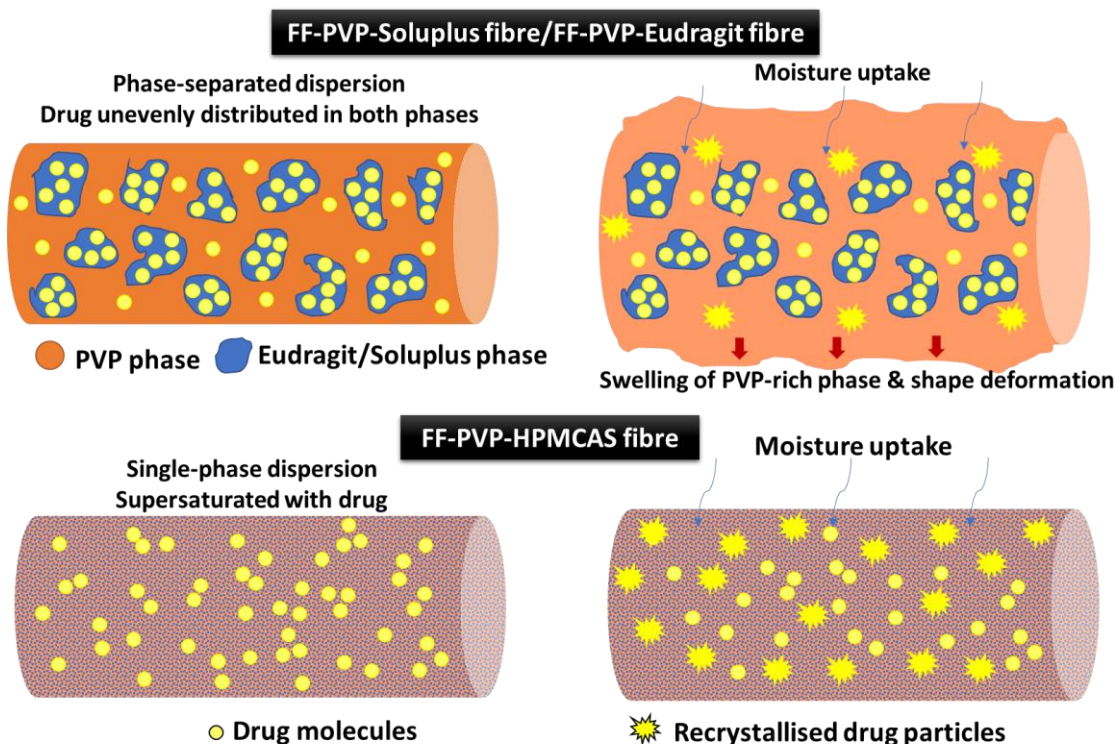


**Figure 11** Illustration of the proposed possible mechanisms phase separation of FF-polymer blend formulations and the drug recrystallisation after moisture sorption.

#### 4. Conclusion

PVP which is a highly processible by electrospinning, but hygroscopic, was successfully blended with a range of non-hygroscopic polymers that are either miscible or partially miscible with PVP. This led to the different degrees phase separation in the polymer blend formulations. The dissolution rates of FF in the ES fibre dispersions were significantly enhanced compared to the pure crystalline material in all formulations. The release rates of the drug showed a clear dependency on the solubility of the polymer in the dissolution media. Moisture sorption was a significant cause of physical instability of the ES PVP based fibres. By blending PVP with other non-hygroscopic polymers, the moisture uptake of the ES fibres can be significantly reduced, and the kinetics involves two processes. However, swelling and physical deformation of the fibres and the mats still occurred for the blends that had significant phase separation.

Although the single-phase FF-PVP-HPMCAS blends showed least physical deformation, they exhibited highest tendency of FF recrystallisation due to the poor miscibility of FF in both PVP and HPMCAS. The results of this study demonstrated that polymer blends can be used as an effective strategy for reducing moisture uptake of ES fibres, however, care is required to ensure that the improved physical stability does not compromise the enhanced dissolution performance of the ES fibres. This study highlighted that using drug-polymer and polymer-polymer miscibility as the guide to carefully select polymeric excipients is highly critical to achieve the balance between maintaining dissolution enhancement, physical stability and deformation of solid dispersion ES fibres against humidity.

### **Declaration of interest**

The authors report no conflicts of interest. The authors alone are responsible for the content and writing of this article.

### **Acknowledgement**

This project has received funding from the Interreg 2 Seas programme 2014-2020 cofunded by the European Regional Development Fund under subsidy contract 2S01-059\_IMODE.

### **References**

- [1] Leuner C, Dressman J. Improving drug solubility for oral delivery using solid dispersions. *Eur. J. Pharm. Biopharm.* 2000; 50: 47-60.
- [2] Van den Mooter G. The use of amorphous solid dispersions: A formulation strategy to overcome poor solubility and dissolution rate. *Drug Discovery Today: Technol.* 2012; 9(2): 79-85.
- [3] Huang Z-M, Zhang Y Z, Kotaki M, Ramakrishna S. A review on polymer nanofibers by electrospinning and their applications in nanocomposites. *Compos. Sci. Technol.* 2003; 63(15): 2223-53.
- [4] Munj H R, Nelson M T, Karandikar P S, Lannutti J J, Tomasko D L. Biocompatible electrospun polymer blends for biomedical applications. *J. Biomed. Mater. Res., Part B* 2014; 102(7): 1517-27.
- [5] Richard-Lacroix M, Pellerin C. Molecular Orientation in Electrospun Fibers: From Mats to Single Fibers. *Macromolecules* 2013; 46(24): 9473-93.

- [6] Rutledge G C, Fridrikh S V. Formation of fibers by electrospinning. *Adv. Drug Delivery Rev.* 2007; 59(14): 1384-91.
- [7] Ignatious F, Sun L, *Electrospun amorphous pharmaceutical compositions*. 2004, Smithkline Beecham Corporation
- [8] Ignatious F, Sun L, Lee C-P, Baldoni J. Electrospun nanofibers in oral drug delivery. *Pharm res.* 2010; 27(4): 576-88.
- [9] Casian T, Borbás E, Ilyés K, Démuth B, Farkas A, Rapi Z, et al. Electrospun amorphous solid dispersions of meloxicam: Influence of polymer type and downstream processing to orodispersible dosage forms. *Int. J. Pharm.* 2019; 569: 118593.
- [10] Lopez F L, Shearman G C, Gaisford S, Williams G R. Amorphous formulations of indomethacin and griseofulvin prepared by electrospinning. *Mol. Pharm.* 2014; 11(12): 4327-38.
- [11] Nagy Z K, Balogh A, Vajna B, Farkas A, Patyi G, Kramarics Á, et al. Comparison of electrospun and extruded soluplus®-based solid dosage forms of improved dissolution. *J. Pharm. Sci.* 2012; 101(1): 322-32.
- [12] Yu D-G, Shen X-X, Branford-White C, White K, Zhu L-M, Bligh S A. Oral fast-dissolving drug delivery membranes prepared from electrospun polyvinylpyrrolidone ultrafine fibers. *Nanotechnology* 2009; 20(5): 055104.
- [13] Marsac P J, Rumondor A C, Nivens D E, Kestur U S, Stanciu L, Taylor L S. Effect of temperature and moisture on the miscibility of amorphous dispersions of felodipine and poly (vinyl pyrrolidone). *J. Pharm. Sci.* 2010; 99(1): 169-85.
- [14] Rumondor A C, Marsac P J, Stanford L A, Taylor L S. Phase behavior of poly (vinylpyrrolidone) containing amorphous solid dispersions in the presence of moisture. *Mol. Pharm.* 2009; 6(5): 1492-505.
- [15] Sethia S, Squillante E. Solid dispersion of carbamazepine in PVP K30 by conventional solvent evaporation and supercritical methods. *Int. J. Pharm.* 2004; 272(1): 1-10.
- [16] Lee J H, Kim M J, Yoon H, Shim C R, Ko H A, Cho S A, et al. Enhanced dissolution rate of celecoxib using PVP and/or HPMC-based solid dispersions prepared by spray drying method. *J. Pharm. Invest.* 2013; 43(3): 205-13.
- [17] Sharma A, Jain C P. Preparation and characterization of solid dispersions of carvedilol with PVP K30. *Res. Pharm. Sci.* 2010; 5(1): 49-56.
- [18] Djuris J, Nikolakakis I, Ibric S, Djuric Z, Kachrimanis K. Preparation of carbamazepine–Soluplus® solid dispersions by hot-melt extrusion, and prediction of drug–polymer miscibility by thermodynamic model fitting. *Eur. J. Pharm. Biopharm.* 2013; 84(1): 228-37.
- [19] Rumondor A C, Stanford L A, Taylor L S. Effects of polymer type and storage relative humidity on the kinetics of felodipine crystallization from amorphous solid dispersions. *Pharm Res* 2009; 26(12): 2599-606.
- [20] Alshahrani S M, Lu W, Park J-B, Morott J T, Alsulays B B, Majumdar S, et al. Stability-enhanced Hot-melt Extruded Amorphous Solid Dispersions via Combinations of Soluplus® and HPMCAS-HF. *AAPS PharmSciTech* 2015; 16(4): 824-34.
- [21] Yang Z, Nollenberger K, Albers J, Craig D, Qi S. Microstructure of an Immiscible Polymer Blend and Its Stabilization Effect on Amorphous Solid Dispersions. *Mol. Pharm.* 2013; 10(7): 2767-80.
- [22] Al-Zoubi N, Odah F, Obeidat W, Al-Jaberi A, Partheniadis I, Nikolakakis I. Evaluation of Spironolactone Solid Dispersions Prepared by Co-Spray Drying With Soluplus (R) and Polyvinylpyrrolidone and Influence of Tableting on Drug Release. *J Pharm Sci* 2018.

- [23] Marks J A, Wegiel L A, Taylor L S, Edgar K J. Pairwise Polymer Blends for Oral Drug Delivery. *J. Pharm. Sci.* 2014; 103(9): 2871-83.
- [24] Alsulays B B, Park J-B, Alshehri S M, Morott J T, Alshahrani S M, Tiwari R V, et al. Influence of molecular weight of carriers and processing parameters on the extrudability, drug release, and stability of fenofibrate formulations processed by hot-melt extrusion. *J. Drug Delivery Sci. Technol.* 2015; 29: 189-98.
- [25] Lu Q, Zografi G. Phase Behavior of Binary and Ternary Amorphous Mixtures Containing Indomethacin, Citric Acid, and PVP. *Pharm. res.* 1998; 15(8): 1202-6.
- [26] Couchman P R, Karasz F E. A Classical Thermodynamic Discussion of the Effect of Composition on Glass-Transition Temperatures. *Macromolecules* 1978; 11(1): 117-9.
- [27] Greenhalgh D J, Williams A C, Timmins P, York P. Solubility parameters as predictors of miscibility in solid dispersions. *J. Pharm. Sci.* 1999; 88(11): 1182-90.
- [28] Forster A, Hempenstall J, Tucker I, Rades T. Selection of excipients for melt extrusion with two poorly water-soluble drugs by solubility parameter calculation and thermal analysis. *Int. J. Pharm.* 2001; 226(1): 147-61.
- [29] Gordon M, Taylor J S. Ideal copolymers and the second-order transitions of synthetic rubbers. i. non-crystalline copolymers. *J. Appl. Chem.* 1952; 2(9): 493-500.
- [30] Taylor L S, Zografi G. Sugar-polymer hydrogen bond interactions in lyophilized amorphous mixtures. *J. Pharm. Sci.* 1998; 87(12): 1615-21.
- [31] Heinz A, Gordon K C, McGoverin C M, Rades T, Strachan C J. Understanding the solid-state forms of fenofibrate—a spectroscopic and computational study. *Eur. J. Pharm. Biopharm* 2009; 71(1): 100-8.
- [32] Kamble RN, Gaikwad S, Maske A, Patil SS. Fabrication of electrospun nanofibres of BCS II drug for enhanced dissolution and permeation across skin. *J. Adv. Res.* 2016; 7(3): 483-489.
- [33] Adeli E. Irbesartan-loaded electrospun nanofibers-based PVP K90 for the drug dissolution improvement: Fabrication, in vitro performance assessment, and in vivo evaluation. *J. Appl. Polym. Sci.* 2015; 132:42212.
- [34] Torres-Martínez E J, Vera-Graziano R, Cervantes-Uc JM, Bogdanchikova N, Olivás-Sarabia A, Valdez-Castro R, Serrano-Medina A, Iglesias AL, Pérez-González GL, Cornejo-Bravo JM, Villarreal-Gómez LJ. Preparation and characterization of electrospun fibrous scaffolds of either PVA or PVP for fast release of sildenafil citrate. *e-Polymers* 2020; 20: 746–758.
- [35] Begum SKR, Varma MM, Raju DB, Prasad RGSV, Phani AR, Jacob B, Salins PC. Enhancement of dissolution rate of piroxicam by electrospinning technique. *Adv. Nat. Sci: Nanosci. Nanotechnol.* 2012; 3:045012.
- [36] Sui X, Chu Y, Zhang J, Zhang H, Wang H, Liu T, Han C. The Effect of PVP Molecular Weight on Dissolution Behavior and Physicochemical Characterization of Glycyrrhetic Acid Solid Dispersions, *Adv. Polym. Technol.* 2020; Article ID 8859658.
- [37] Franco P, De Marco I. The Use of Poly(N-vinyl pyrrolidone) in the Delivery of Drugs: A Review. *Polymers (Basel).* 2020;12(5):1114.
- [38] Wang C, Ma C, Wu Z, et al. Enhanced Bioavailability and Anticancer Effect of Curcumin-Loaded Electrospun Nanofiber: In Vitro and In Vivo Study. *Nanoscale Res Lett.* 2015;10(1):439.
- [39] Sriyanti I, Edikreshna D, Rahma A, Munir MM, Rachmawati H, Khairurrijal K. Mangosteen pericarp extract embedded in electrospun PVP nanofiber mats: physicochemical properties and release mechanism of  $\alpha$ -mangostin. *Int. J. Nanomedicine.* 2018;13:4927-4941.

- [40] Tort S, Yıldız A, Tuğcu-Demiröz F, Akca G, Kuzukıran Ö, Acartürk F. Development and characterization of rapid dissolving ornidazole loaded PVP electrospun fibers. *Pharm. Dev. Technol.* 2019;24(7):864-873.
- [41] Chuangchote S, Sagawa T, Yoshikawa S. Electrospinning of poly(vinyl pyrrolidone): Effects of solvents on electrospinnability for the fabrication of poly(p-phenylene vinylene) and TiO<sub>2</sub> nanofibers. *J. Appl. Polym. Sci.* 2009; 114(5): 2777-2791.
- [42] Zhang M, Li H, Lang B, O'Donnell K, Zhang H, Wang Z, et al. Formulation and delivery of improved amorphous fenofibrate solid dispersions prepared by thin film freezing. *Eur. J Pharm. Biopharm.* 2012; 82(3): 534-44.
- [43] Waterman K C, Adami R C. Accelerated aging: Prediction of chemical stability of pharmaceuticals. *Int. J Pharm.* 2005; 293(1): 101-25.
- [44] Démuth B, Farkas A, Szabó B, Balogh A, Nagy B, Vágó E, et al. Development and tableting of directly compressible powder from electrospun nanofibrous amorphous solid dispersion. *Adv. Powder Technol.* 2017; 28(6): 1554-63.
- [45] Al-Muhtaseb A H, McMinn W A M, Magee T R A. Moisture Sorption Isotherm Characteristics of Food Products: A Review. *Food Bioprod. Process.* 2002; 80(2): 118-28.
- [46] Anderade P R D, Lemus M R, Perez C C E. Model of Sorption Isotherms for Food: Uses and Limitation. *Vitae* 2011; 18: 325-34.
- [47] Qi S, Belton P, McAuley W, Codoni D, Darji N. Moisture uptake of polyoxyethylene glycol glycerides used as matrices for drug delivery: kinetic modelling and practical implications. *Pharm. Res.* 2013; 30(4): 1123-36.
- [48] Lewicki P P. The applicability of the GAB model to food water sorption isotherms. *Int. J. Food Sci. Technol.* 1997; 32(6): 553-7.
- [49] Hunter N E, Frampton C S, Craig D Q M, Belton P S. The use of dynamic vapour sorption methods for the characterisation of water uptake in amorphous trehalose. *Carbohydr. Res.* 2010; 345(13): 1938-44.
- [50] Waterman K C, Adami R C. Accelerated aging: Prediction of chemical stability of pharmaceuticals. *Int. J. Pharm.* 2005; 293(1-2): 101-25.
- [51] Turner D T, Schwartz A. The glass transition temperature of poly(N-vinyl pyrrolidone) by differential scanning calorimetry. *Polymer* 1985; 26(5): 757-62.
- [52] Callahan J C, Cleary G W, Elefant M, Kaplan G, Kensler T, Nash R A. Equilibrium Moisture Content of Pharmaceutical Excipients. *Drug Dev. Ind. Pharm.* 1982; 8(3): 355-69.